

BBA 42049

The extent of energy transfer among Photosystem II reaction centers in *Chlorella*

Arthur C. Ley and David C. Mauzerall

The Rockefeller University, 1230 York Avenue, New York, NY 10021 (U.S.A.)

(Received April 8th, 1986)

Key words: Energy transfer; Reaction center; Photosystem II; Fluorescence induction; (*Chlorella*)

We have investigated the extent of energy transfer among Photosystem II reaction centers in *Chlorella vulgaris*. The cells show typical non-exponential fluorescence induction kinetics in the presence of the herbicide 3-(3,4-dichlorophenyl)-1,1-dimethylurea. We used single-turnover flashes to determine effective absorption cross-sections for Photosystem II reaction centers (RCII) in cells which were simultaneously illuminated with a continuous background light. We varied the background irradiance to control the fraction, γ , of the total RCII closed at the time of a flash. We found that the absorption cross-section per RCII was almost completely independent of γ . Relative oxygen flash yields measured at low laser flash energies were similarly unaffected when RCII were closed with the background light. We simultaneously measured laser flash energy saturation curves for oxygen production and for the increase in fluorescence quantum yield measured 30 μ s after the laser flash. The oxygen and fluorescence saturation curves were almost identical. We conclude from these results and appropriate theoretical calculations that the difference in the probabilities for escape of excitation energy at open and closed RCII is small (under 0.25). No matter how many RCII share a common antenna, closing RCII does not greatly change the absorption cross-section of the remaining open RCII. Either the probability for escape from closed traps is small, or the probabilities for escape from open and closed traps are nearly equal.

Introduction

The vast majority of the photosynthetic pigments in plants function to absorb light and transfer the energy to reaction centers (RC): sites where the photochemical reactions of photosynthesis occur. RCs are generally present in the photosynthetic apparatus in the ratio of 1 RC per 100–500 total pigment molecules [1–7]. Functional antenna sizes for RCI or RCII have been approximated from relative rates of photochemical reactions

[5,6,8,9] or determined directly from measurements of absorption cross-sections [10–12]. Functional antenna sizes range from 50 to 400 pigment molecules, depending on the RC, organism and growth conditions [5–12].

There are now several lines of evidence suggesting that more than one RCII may share a common pool of antenna molecules. Experimental support for such 'multi-units' comes from measurements of fluorescence induction [9,13–18] and the effects of added fluorescence quenchers [19,20], changes in fluorescence yields measured on the nano- and picosecond time-scales [21–23], rates of O₂ production [6,14,24], and effective absorption cross-sections [12]. Typically, 3–5 RCII are believed to share an antenna [9,12–14,23–25].

Abbreviations: RCII, reaction center of Photosystem II; RCI, reaction center of Photosystem I; DCMU, 3-(3,4-dichlorophenyl)-1,1-dimethylurea; Y_{O₂}, relative oxygen flash yield; Chl, chlorophyll.

The major physiological effect of the organization of RCII and their antennae into multi-centered units is believed to be manifest when some fraction of the RCII in the unit are 'closed' and unable to use absorbed light energy for photochemistry. Under these conditions it has been thought [9,13,14,17,20,24] that light energy arriving initially at the closed RCII can continue on to be used by other open RCII in the unit. Thus, the effective absorption cross-section for an open RCII should increase as the fraction of closed RCII in a unit increases. Evidence in support of such energy exchange among RCII derives from experiments in which the rate of some photochemical reaction (e.g., O_2 production or changes in fluorescence yield) is related to the fraction of open RCII [13–18]. These experiments are usually performed with an inhibitor, such as DCMU, present to block secondary electron transfer events [4,5,8,9,13–18,24,25]. In general, the probability for energy transfer among RCII derived from such measurements is quite high (over 0.7) [25].

We have recently described the results of experiments in which we measured the flash energy saturation behavior of O_2 yields from algae illuminated with single-turnover flashes of laser light [10–12]. We found that the data were well described by the cumulative one-hit Poisson distribution. This result, obtained in the absence of herbicides, implies that the absorption cross-section for open RCII does not change greatly as the fraction of closed RCII in the sample increases.

In this report we describe the results of several experiments to test whether closing some fraction of the RCII present in *Chlorella* cells influences the effective absorption cross-section for the remaining open RCII. We find that the measured absorption cross-section is almost completely independent of the fraction of closed RCII. A strong conclusion based on our results is that the difference between the rates of quenching of excitation energy at open and at closed RCII is small.

Materials and Methods

We grew batch cultures of the green alga *Chlorella vulgaris* at 20°C in continuous light from fluorescent lamps [10]. We collected cells by centrifugation and resuspended the cells in fresh

growth medium. We determined Chl concentrations from the absorbance of ethanol extracts of the cells and the equations of Winternans and DeMots [26]. For all the experiments described in this report, we used suspensions of cells (Chl concentrations between 50 and 100 μ M, see figure legends) which had settled onto the surface of the bare Pt electrode of the O_2 polarograph [10]. The settled cells covered less than 50% of the electrode surface. Growth media supplemented by 10 mM $NaHCO_3$ flowed at 5–10 ml/min over the dialysis membrane covering the cells.

We measured flash energy saturation curves for O_2 production in the absence of background illumination as described previously [10,11]. To determine the effects of background irradiance on absorption cross-sections, we illuminated the cells with two sources of light. The first was the train (0.5 or 0.2 Hz, see figure legends) of 596 nm, 0.5 μ s (total duration) flashes of light from a flashlamp-pumped dye laser (Phasar DL2100C). The second was a continuous 580 nm or 650 nm (see figure legends) background light from a 500 W projection lamp filtered with combinations of bandpass and interference filters. We varied the background irradiance by changing the lamp voltage. The laser and the continuous light were directed onto the algae with a dual-armed fiber-optics light pipe with the common end positioned 3 mm above the Pt electrode surface.

We performed simultaneous measurements of O_2 flash yields Y_{O_2} and fluorescence yields ($\Delta\phi(F30)$) as described previously [11]. All Y_{O_2} were calculated as the ratio of the O_2 yield of the first attenuated flash to the yield of saturating steady-state flashes.

We measured room-temperature fluorescence induction kinetics from cells on the Pt electrode illuminated with continuous light. We obtained 580 nm light from the output of a 6 V tungsten-iodide lamp which we focused through bandpass and interference filters into one arm of the fiber-optics light pipe. We initiated illumination via an electromechanical shutter (Vincent Associates.) with an opening time less than 1 ms. We collected fluorescence from the algae with the common end of the light pipe and presented it, via the second arm of the light pipe, to a photomultiplier tube (Hamamatsu R262) protected with long

pass (over 660 nm) filters and a 680 nm interference filter. The converted photomultiplier current was captured with a Biomation 802 digitizer and read out on a strip chart recorder. The response time of this apparatus was 0.3 ms.

We dark-adapted the *Chlorella* cell suspensions for 25 min prior to the start of the fluorescence induction experiments. We added DCMU from an aqueous stock solution to the suspensions after the dark-adaptation period. We then placed the cell suspensions on the electrode surface. After an additional dark period during which the cells settled onto the Pt electrode surface (times between 2 and 30 min gave identical results), we illuminated the cells and recorded the fluorescence induction kinetics. We performed all manipulations prior to actinic illumination in complete darkness.

We calculated flash energy saturation curves using a modified version to the iterative semiannihilation algorithm of Mauzerall [23] as described in the Appendix.

Results and Conclusions

Fluorescence induction

The extent of energy transfer among RCII is commonly estimated from the analysis (Fig. 1) of the rise in fluorescence yield observed when dark-adapted, DCMU-poisoned cells of chloroplasts are illuminated with continuous light [9,13–18,25]. The data shown in Fig. 1 confirm the results repeatedly obtained by others [5,9,13–18,25,27–30]. We also see no substantial contribution of a slow component to the fluorescence rise kinetics (Fig. 1a). This component has been reported to be small (about 15% [27]) or absent [20] in *Chlorella*.

A semilogarithmic plot of the fraction of the total area above the fluorescence rise curve removed during the induction process ('area', Fig. 1B) shows that in *Chlorella*, similar to many other reports [5,8,9,13–18,30]. 'area' growth is not a first-order process, but instead accelerates with time. Melis and co-workers [8,9,15–17] have inferred from similar data that the effective absorption cross-section for an open RCII increases 3- to 5-fold as RCII close during induction. However, the assumption that the fluorescence yield on this time-scale is exclusively controlled by the redox state of RCII is a potential source of error (see below).

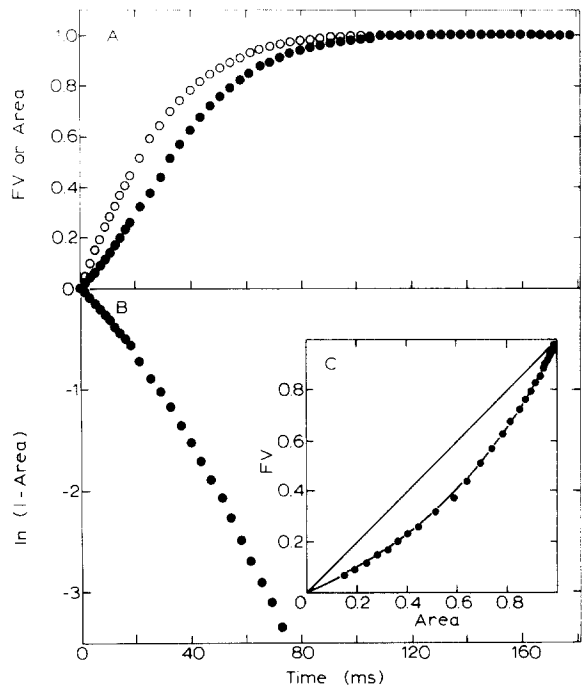


Fig. 1. Kinetic analysis of the increase in fluorescence emission from *C. vulgaris* cells illuminated at room temperature in the presence of DCMU. Dark-adapted cells (Chl/cell = 0.36 fmol, Chl *b*/Chl *a* = 0.26) were suspended at a Chl concentration of 70 μ M in growth medium containing 14 μ M DCMU. The actinic irradiance (580 nm) was $2 \cdot 10^{15}$ quanta/cm² per s. Fluorescence emission was measured at 680 nm. (A) Plots of the kinetics of the increase in relative fluorescence yield (F_v , closed circles) and of the growth in relative area above the fluorescence rise curve ('area', open circles) during continuous illumination of dark adapted cells. In this measurement, the ratio of the initial minimal value of the relative fluorescence yield (F_0) to the final maximal value (F_m) was: $F_m/F_0 = 3.6$. F_m was constant for at least 10 s of continuous irradiation. (B) A semi-logarithmic plot of the kinetics of the increase in 'area' shown in A). (C) A plot of F_v as a function of 'area'. The data are from (A). The solid curve through the data was calculated using Eqn. 1 with $p = 0.55$ as described in the text.

The common estimate of the extent of energy transfer among RCII is obtained from the fit of the variable fluorescence (F_v) to Eqn. 1 [13, 14,18,25]:

$$F_v = (1 - p)q / (1 - pq) \quad (1)$$

where q is the fraction of closed RCII and p , the 'connection factor' [13,18,25], is the probability for the transfer of an excitation encountering a closed RCII to another RCII. The correction for p

introduced by Paillotin [25,31,32]:

$$P = p(F_m / (F_m + F_0)) \quad (2)$$

is of doubtful value, since it is based on the assumption that F_v arises solely from an increase in exciton lifetime on closing RCII. Recent measurements of fluorescence lifetimes contradict this assumption [33,34].

Using the assumptions stated previously, a fit of Eqn. 1 to the plot of F_v vs. 'area' ($=q$) will yield a value for p . The best fit of our data (Fig. 1C) gives $p = 0.55$.

Our intention here is to show that our strain of *Chlorella* and our measurements of fluorescence induction kinetics yield results quite analogous to those obtained by others using a variety of organisms [4,5,8,9,13–25]. We will now contrast these results with results obtained using a far more direct measurement of RCII photochemistry and antenna size.

Flash saturation curves

Another approach to this problem, which we will use in the remainder of this report, uses single-turnover flashes of light rather than continuous illumination, avoids the use of herbicides, and directly measures the product of RCII photochemistry, O_2 . We shall use the terms defined as follows. T is the number of RCII that share an antenna. The T RCII plus their antenna comprise a Unit. σ_u is the total absorption cross-section (RC plus antenna) for the Unit at the wavelength of the assaying laser flash. $\sigma = \sigma_u/T$ is the absorption cross-section per RCII. An RCII is 'open' if it can perform photochemistry when visited by an excitation and is 'closed' if it cannot. γ is the fraction of the total RCII in a sample which are open at the time of a flash. We define A as the probability that an excitation encountering a closed RCII can escape to a location in the Unit where it has an equal probability of finding any RCII in the Unit, i.e., it is as random as the original excitation. B is the similarly defined probability of escape from an open RCII. We assume that the probabilities A and B are independent of γ .

The definitions of A and B allow use to the simple algorithm described in the Appendix to

calculate the fate of excitations absorbed in Units in which some fraction of the RCII are closed. Note that the detailed path of the excitation is ignored. The statement $A = 0$ does not necessarily imply that an excitation encountering a closed RCII cannot leave the RCII or its vicinity; only that the excitation does not encounter another RCII during its lifetime. Likewise, the values of A and B imply nothing about the number of times an excitation may visit the same RCII, be it open or closed. The probability of escape of an excitation from a RCII is a concept whose apparent simplicity is rather deceptive. It is similar to the problem of diffusion to an imperfect sink. Collins and Kimball [36] have shown that in this case the picture of the escape probability as a reflection coefficient is inconsistent. Thus the need for the specific definitions given above.

In general, the flash saturation behavior for a product of RCII photochemistry (e.g., O_2) will depend on the values of T , A and B . However, if $A = B$, the relationship between flash energy and flash yield is very close to the cumulative one-hit Poisson distribution [10,23]. Assuming uniform illumination conditions and antenna sizes.

$$Y = 1 - \exp(-\phi\sigma_u E/T) \quad (3)$$

where Y is the relative yield of the measured product of RCII photochemistry and E is the energy density (quanta/area) at the sample of the single-turnover, monochromatic flash. ϕ is the quantum yield for primary photochemistry by an open RCII. Eqn. 3 is valid, as long as $A = B$, for any T , from the separate package case ($T = 1$) to an infinite matrix. In practice, the fit of Eqn. 3 to experimentally determined values for some product of RCII photochemistry, such as O_2 flash yields, gives $\sigma_{O_2} = \phi\sigma$, the effective absorption cross section per RCII as assayed by (in this case) O_2 production. Since $\phi > 0.95$ [37–39], $\sigma_{O_2} \approx \sigma$. Measurement at steady-state flash excitation ensures that one measures an average overall S states.

If $A \neq B$, Eqn. 3 will not describe the flash saturation behavior of Y_{O_2} . The shape of the saturation curve will now depend on the values of T , A and B [23]. Fig. 2A shows curves calculated (using the iterative method described in the Appendix) for various values of T (curves '1') and A

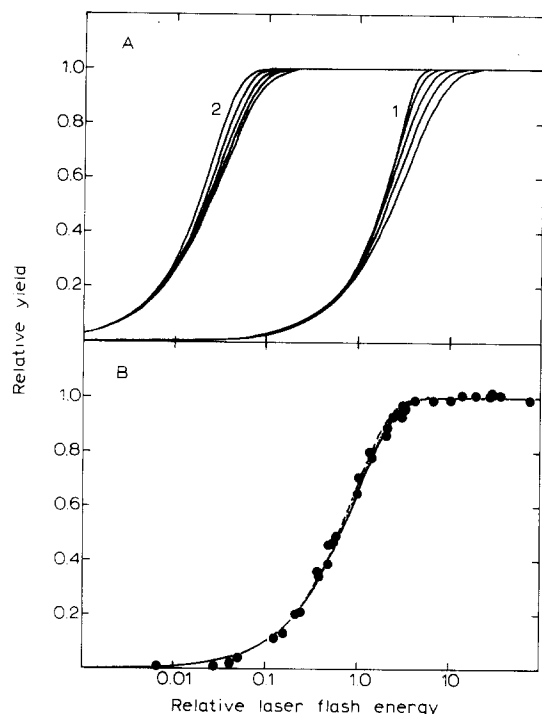


Fig. 2. Effects of energy transfer among RCII on the shape of the flash saturation curve for O_2 production. (A) Calculation of flash saturation curves for different values of T and A . Curves '1': $\sigma = 0.3$, $A = 0.9$, $B = 0$, and from right to left $T = 1, 2, 4, 10, 50$. Curves '2': $T = 4$, $\sigma = 30$, $B = 0$, and from right to left, $A = 0.025, 0.50, 0.75, 1.0$. Note that the different values for σ simply shift the curves along the flash energy axis. (B) A fit of calculated flash saturation curves to O_2 flash yield data. The data were obtained from *Chlorella* cells ($Chl/cell = 0.40$ fmol, $Chl\ b/Chl\ a = 0.31$) illuminated by a train of 596 nm laser flashes (0.5 Hz) in the absence of any continuous background illumination. The Chl concentration of the cell suspension was $90\ \mu M$. A relative laser flash energy of 1.0 corresponds to 1.110^{14} quanta/cm 2 . Solid curve: $\sigma_{O_2} = 95\ \text{\AA}^2$, $A = B = 0$. Dashed curve: $T = 4$, $\sigma_{O_2} = 95\ \text{\AA}^2$, $A = 0.25$, $B = 0$. Dotted curve: $T = 50$, $\sigma_{O_2} = 95\ \text{\AA}^2$, $A = 0.10$, $B = 0$.

(curves '2'). For clarity in these calculations, and for comparison with previous work which has ignored B , we have set $B = 0$. We shall specifically consider this important parameter separately (vide infra).

The calculated curves plotted in Fig. 2A show that the effect of increasing either A or T is to produce flash energy saturation curves which are sharper than the exponential behavior described by Eqn. 3. This behavior reflects the rather small

increase in absorption cross-section per open RCII as RCII are closed during the flash. The curves in Fig. 2A are indistinguishable at low values of σE . At these flash energies, Units absorb either one or no photons during a flash. The effects of energy transfer among RCII can only be observed when a Unit absorbs more than one photon during a flash.

Fig. 2B shows flash saturation data for Y_{O_2} . As we have previously reported [10,11], the data are well fit using Eqn. 3. The solid curve in Fig. 2B was calculated using Eqn. 3 with $\sigma_{O_2} = 95\ \text{\AA}^2$.

We have previously noted [10,23] and Paillotin et al. [32] have more recently commented, that the flash saturation curves are only weak functions of T or A . It is possible to fit the data shown in Fig. 2B reasonably well using a range of values for T and A . For example, we calculated the dashed curve in Fig. 2B using $T = 4$ and $A = 0.25$ and the dotted curve with $T = 50$ and $A = 0.1$. For both curves, $\sigma_{O_2} = 95\ \text{\AA}^2$. In general, reasonable fits to the data can be obtained for $T < 10$ provided $TA \leq 1$. For $T > 10$, good fits can be obtained only if $A < 0.1$. Irrespective of the value of T , we cannot obtain good fits to the data using any value for A greater than 0.35.

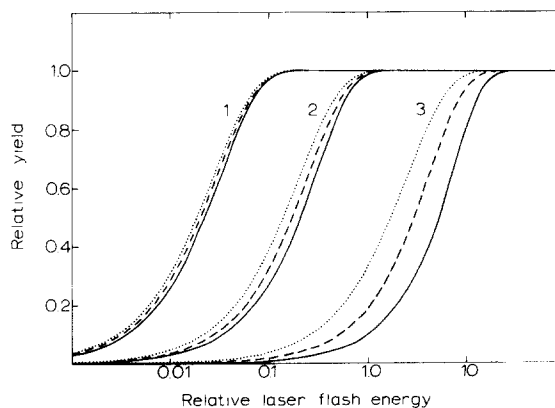


Fig. 3. The effects of 'closed' RCII on the shape of the flash saturation curve for O_2 production. For all three families of curves, $T = 4$ and $B = 0$. Curves '1': $\sigma = 30$, $A = 0.25$. Curves '2': $\sigma = 3.0$, $A = 0.50$. Curves '3': $\sigma = 0.10$, $A = 0.95$. Solid curves were calculated using $\gamma = 1.0$, dashed curves using $\gamma = 0.50$, and dotted curves using $\gamma = 0.05$. The relative maximum yield for all curves has been normalized to unity.

Flash saturation in the presence of closed RCII

From the preceding discussion it is clear that if $B = 0$ and $A > 0$ the effective absorption cross-section per open RCII will increase as the fraction of closed RCII in a Unit increases. Thus, we expect that flash saturation curves measured under conditions where only a fraction, γ , of the RCII in a sample are open at the time of the flash will show the increase in σ .

The calculated curves shown in Fig. 3 demonstrate the expected magnitude of this effect in the case where $T = 4$ and $B = 0$. The three families of curves were calculated using different values for A (from left to right, $A = 0.25, 0.50, 0.95$). A family of curves (solid, dashed and dotted) was calculated for each A using different values for γ (1.0, 0.5 and 0.05, respectively). All curves have been renormalized to a maximum flash yield of unity.

For any value of A , the calculated flash saturation curves are displaced to lower flash energies as γ decreases. The magnitude to which the calculated curves are displaced depends on the values of γ , A and T . Furthermore, the shift to lower

flash energies is exhibited over the entire curve and is not confined to the region near saturation (as is the case for the curves shown in Fig. 2). Thus, the comparison of flash saturation curves for RCII photochemistry measured under conditions where γ is varied experimentally can provide a sensitive test for the presence and magnitude of energy transfer among RCII.

Effects of background illumination

We have determined the flash saturation behavior for Y_{O_2} measured in the presence of a continuous background illumination which we adjusted to control the fraction of open RCII at the time of a laser flash. The data shown in Fig. 4 describe our experimental conditions.

The closed circles in Fig. 4A show the relative rate of steady-state photosynthetic O_2 production (P/P_{max}) by *Chlorella* cells illuminated with a continuous 650 nm background light. The triangles represent values for the relative O_2 yield (Y/Y_{max}) produced by the cells when exposed to a saturating, single-turnover laser flash superim-

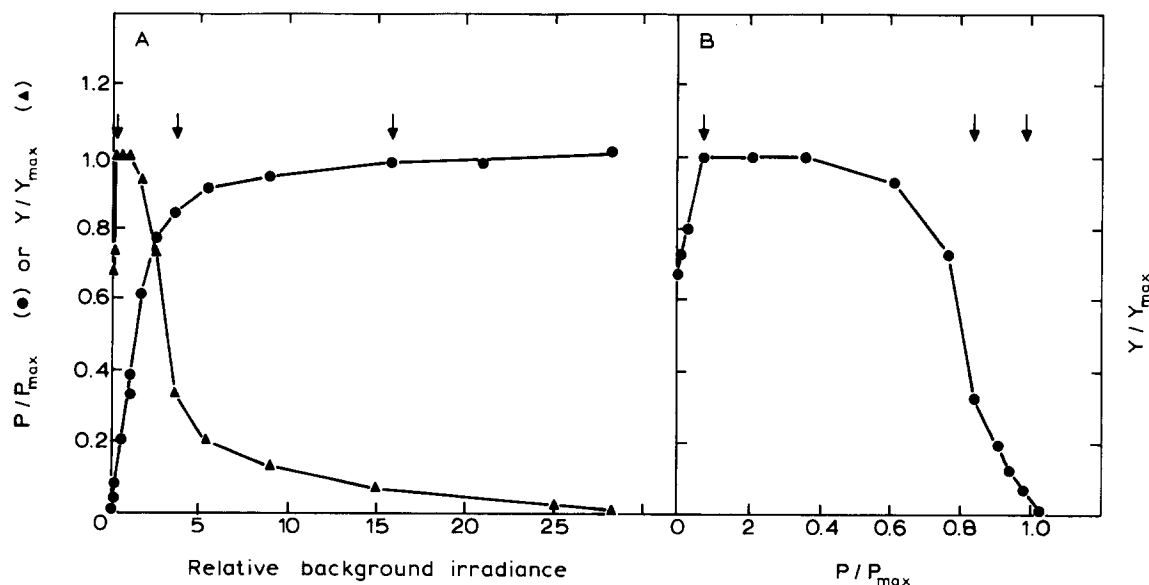


Fig. 4. Relationship between steady-state rates of photosynthesis and O_2 flash yields in *Chlorella* Cells (Chl/cell = 0.33 fmol, Chl b /Chl a = 0.24) were suspended in growth medium at a Chl concentration of 95 μ M. (A) Relative steady-state rates of O_2 production (P/P_{max} , circles) and relative light-saturated O_2 flash yields (Y/Y_{max} , triangles) plotted as functions of the irradiance of a continuous 650 nm background light. Units of background irradiance are $9.7 \cdot 10^{14}$ quanta/cm² per s. (B) Y/Y_{max} plotted as a function of P/P_{max} . The arrows in (A) and (B) indicate points at which the O_2 flash saturation data shown in Fig. 5C,D were obtained.

posed on the continuous background illumination. Both P/P_{\max} and Y/Y_{\max} are plotted as functions of the irradiance of the continuous 650 nm background light. The data in Fig. 4A are replotted in Fig. 4B as Y/Y_{\max} vs. P/P_{\max} .

Values for Y/Y_{\max} increase at low irradiance as the rate of PSII excitation by the background light becomes sufficient to overcome the dark relaxation of the O_2 -evolving system [40]. This effect is caused by the relatively slow rate of excitation (0.5 Hz) provided by the laser. Flash yields remain high during the linear portion of the photosynthesis-irradiance curve, then decrease as photosynthesis becomes light-saturated. The relationship between Y_{O_2} and continuous O_2 production (Fig. 4B) is far from linear. This is because the turnover time for widely separated (more than 0.1 s) single turnover flashes (about 0.5 ms) is much shorter than that for the total throughout of photosynthesis. The data in Fig. 4 indicate that the slow turnover time is at least 5-times as long (about 3 ms) as the flash turnover time. Thus, rates for continuous O_2 production will be nearly light-saturated before large decreases in Y_{O_2} can occur.

Fig. 4 shows that we can use light alone (no herbicides) to adjust the fraction of RCII open during the measurement of a flash saturation curve for Y_{O_2} . The three arrows in Fig. 4 show the values for Y/Y_{\max} , P/P_{\max} , and background irradiance at which we measured the three sets of data shown in Fig. 5C, D.

Fig. 5 shows the results of two sets of experiments to test the effect of closing RCII with continuous background irradiance on the light-saturation behavior of Y_{O_2} . The data shown in Fig. 5C, D were obtained from the experiment using 650 nm background light shown in Fig. 4. The data shown in Fig. 5A, B were obtained from a similar experiment using a 580 nm background light.

Two sets of data are shown in Fig. 5A. Data obtained in the absence of any background illumination are shown by the crosses. The solid circles represent data obtained in the presence of a continuous dim 580 nm background irradiance ($P/P_{\max} = 0.2$) sufficient to produce maximum light-saturated Y_{O_2} ($Y/Y_{\max} = 1.0$). The background illumination has overcome the loss of S_3 due to the low laser pulse frequency (0.5 Hz).

Within experimental error the two sets of data are identical. Thus, the presence of a dim continuous background light does not of itself disturb the shape of the light-saturation curve for Y_{O_2} .

Both sets of data shown in Fig. 5A are replotted as the closed circles in Fig. 5B. The open circles in Fig. 5B represent data obtained in the presence of a 580 nm background irradiance sufficient to close about 75% of the RCII present ($Y/Y_{\max} = 0.25$, $P/P_{\max} = 0.9$).

The data shown in Fig. 5C were obtained under the conditions shown in Fig. 4 such that $Y/Y_{\max} = 1.0$. These data are replotted in Fig. 5D as the solid circles. Data obtained for $Y/Y_{\max} = 0.3$ and $Y/Y_{\max} = 0.07$, $P/P_{\max} = 0.98$ are also shown in Fig. 5D as the crosses and open circles, respectively.

It is clear from the results of the experiments shown in Fig. 5 that there is no large change in the shape of the flash saturation behavior of Y_{O_2} when RCII are closed by the presence of a background illumination. Even when more than 90% of the RCII are closed at the time of a flash (Fig. 5D), the observed saturation behaviors are, to within the scatter in the data, the same. We conclude that if $B = 0$, A is small.

The calculated curves shown in Fig. 5 allow us to determine an upper limit for the value of A . In all four panels of Fig. 5, $T = 4$ and solid curves were calculated using $A = 0$, dashed curves with $A = 0.25$, and dotted curves with $A = 0.50$. The curves drawn through the data in Fig. 5A, C were fit to the data by adjusting the value for σ_{O_2} used in the calculations. For these curves we have assumed $\gamma = 1.0$ (all RCII are open). Values of σ_{O_2} obtained from these fits are 5–10% smaller when $A > 0$ than when $A = 0$.

The curves shown in Fig. 5B and Fig. 5D were calculated using the values for σ_{O_2} and A obtained from the fits to the data shown in Fig. 5A and Fig. 5C, respectively. Values for γ were determined by the measured values of Y/Y_{\max} . $\gamma = 0.25$ for the curves shown in Fig. 5B and $\gamma = 0.07$ for the curves shown in Fig. 5D. Thus all the parameters used to calculate the curves shown in Fig. 5B and Fig. 5D are fixed by the initial fits to the data for $\gamma = 1.0$ and by the measured values for Y/Y_{\max} . No independently adjustable parameters are used.

For both sets of experiments shown in Fig. 5,

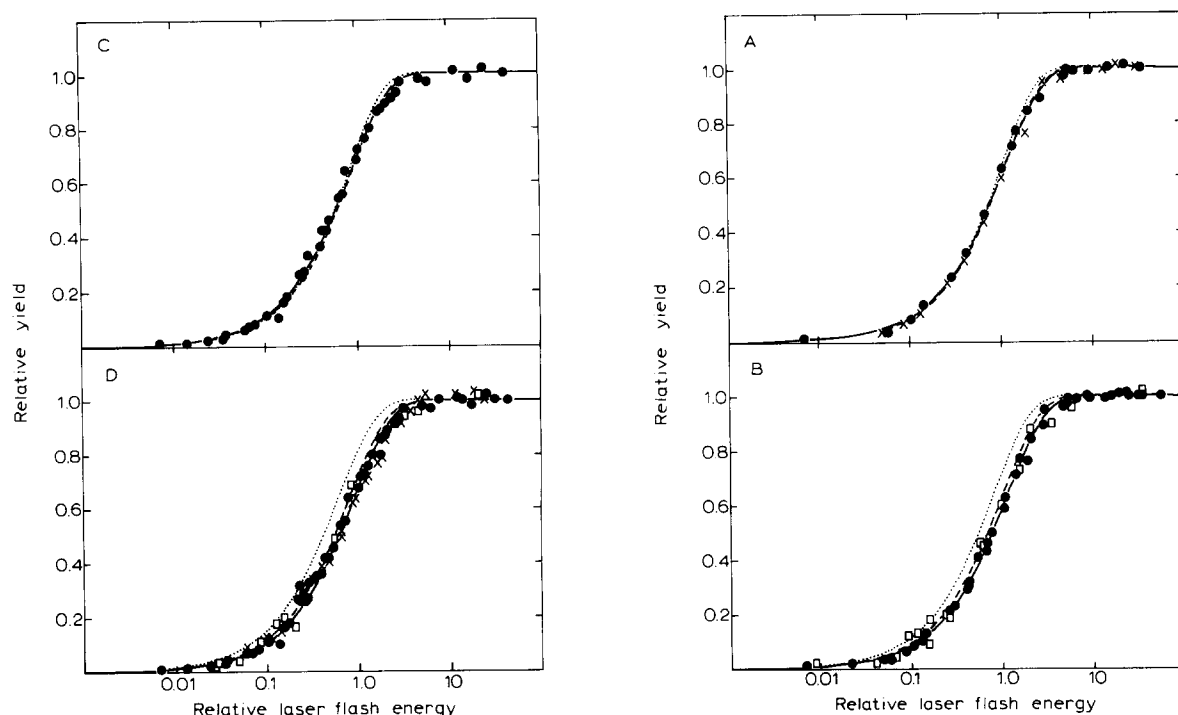


Fig. 5. Effects of continuous background illumination on O_2 flash saturation behavior in *Chlorella*. (A) O_2 flash yields measured from cells in the presence (closed circles, $Y = Y_{\max}$) and in the absence (crosses, $Y = 0.85 Y_{\max}$) of a continuous dim 580 nm background illumination. The laser flash frequency was 0.5 Hz for both sets of data. The background irradiance was $6.9 \cdot 10^{14}$ quanta/cm² s. A relative laser flash energy of 1.0 corresponds to $1.1 \cdot 10^{14}$ quanta/cm². Cells (Chl/cell = 0.33 fmol, Chl *b*/Chl *a* = 0.26) were suspended in growth medium at a Chl concentration of 63 μ M. Solid curve: $T = 4$, $\sigma_{O_2} = 81 \text{ \AA}^2$, $A = B = 0$, $\gamma = 1.0$. Dashed curve: $T = 4$, $\sigma_{O_2} = 77 \text{ \AA}^2$, $A = 0.25$, $B = 0$, $\gamma = 1.0$. Dotted curve: $T = 4$, σ_{O_2} , $A = 0.50$, $B = 0$, $\gamma = 1.0$. (B) All the data from (A) are replotted as the solid circles. The open circles ($Y = 0.25 Y_{\max}$) represent data obtained from the same cells used in (A), co-illuminated with a continuous, bright ($47 \cdot 10^{14}$ quanta/cm² per s), 580 nm background light. Laser flash frequency and energies are as in (A). The three curves were calculated as in (A) except that $\gamma = 0.25$. (C) Laser flash energy dependence of Y_{O_2} from *Chlorella* co-illuminated with a continuous dim 650 nm background light ($Y = Y_{\max}$). Cells and Chl concentration are the same as in Fig. 4. The background irradiance was $2.4 \cdot 10^{14}$ quanta/cm²; the laser flash frequency was 0.2 Hz. A relative flash energy of 1.0 corresponds to $1.1 \cdot 10^{14}$ quanta/cm² per s. Solid curve: $T = 4$, $\sigma_{O_2} = 86 \text{ \AA}^2$, $A = B = 0$, $\gamma = 1.0$. Dashed curve: $T = 4$, $\sigma_{O_2} = 79 \text{ \AA}^2$, $A = 0.25$, $B = 0$, $\gamma = 1.0$. Dotted curve: $T = 4$, $\sigma_{O_2} = 79 \text{ \AA}^2$, $A = 0.5$, $B = 0$, $\gamma = 1.0$. (D) Effects of continuous 650 nm background illuminations of varied irradiance on the laser flash energy dependences of Y_{O_2} from *Chlorella* cells. Laser flash frequency and energies are as in (C). Closed represent data from cells co-illuminated with bright continuous 650 nm light ($23 \cdot 10^{14}$ quanta/cm² per s, $Y = 0.30 Y_{\max}$). Open circles represent data from cells co-illuminated with very bright ($110 \cdot 10^{14}$ quanta/cm² per s, $Y = 0.07 Y_{\max}$) 650 nm light. The three curves were calculated as in (C), except that $\gamma = 0.07$.

$A = 0.50$ clearly does not fit the data. $A = 0.25$ appears to be an upper limit for A in both cases. Even for values of T as low as 2, good fits could not be obtained with values of A greater than 0.35. We conclude from the experiments shown in Fig. 5, that if $B = 0$, A is small, i.e., less than 0.25 if more than two RCII share an antenna.

It has been suggested to us that our use of a strong background illumination to close RCII may have induced a decrease in the PSII antenna size through the reduction of the plastoquinone pool due to the strong light and resulting activation of

a protein kinase [41,42]. The smaller PSII antenna size could have compensated for the anticipated increase in observed cross-section due to energy transfer. We note that for $p \approx 0.6$, a substantial decrease (about 50%) in antenna size would be required to account for the results shown in Fig. 5. When changes in apparent RSII antenna size have been reported for green algae or isolated chloroplasts from higher plants, they have been small (about 15%) [43–45]. Furthermore, such results have been obtained from experiments specifically designed to maximize changes in high and low

continuous irradiances would not have optimized the hypothesized differences in PSII antenna size.

To test for changes in PSII antenna size induced by the process discussed above, we measured σ_{O_2} in cells illuminated with a dim 580 nm background light ($Y/Y_{\max} = 1.0$). We next illuminated these cells with a bright background light ($Y/Y_{\max} = 0.1$) and remeasured σ_{O_2} after 30 min, in the presence of the bright light. Finally, we decreased the background irradiance to the original low level and measured σ_{O_2} at 2, 2, 30 and 60 min following the end of the bright illumination period. Similar to the results shown in Fig. 5, we

could find no difference among any of the measurements, either in the shape of the flash saturation curve or in σ_{O_2} (data not shown).

The phosphorylation of the Chl *a/b* light-harvesting protein has been shown to be reversible with a half-time, in the dark, of 5–10 min [44,45,47]. Since we see no difference in σ_{O_2} measured before, during or after bright illumination, we conclude that under our conditions, any changes in PSII antenna size due to reversible, light-induced protein phosphorylation events are small (under 10%) and do not significantly influence the results shown in Fig. 5 or conclusions derived from them.

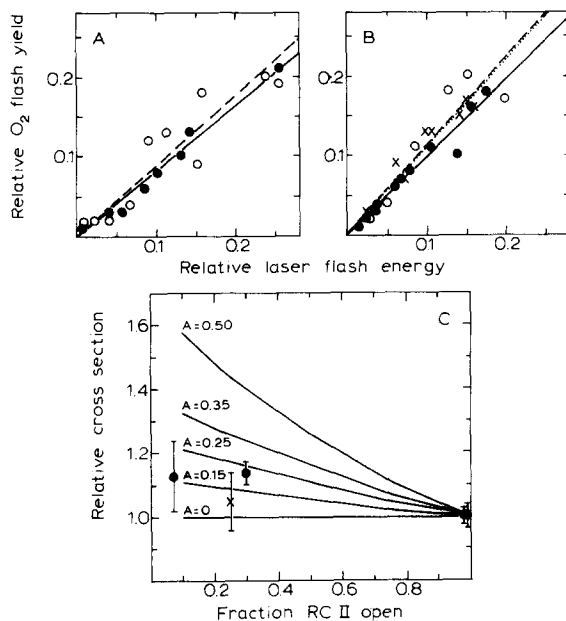


Fig. 6. (A) Linear regressions on the low laser flash energy portion of the data shown in Fig. 5B. Symbols and flash energies are the same as in Fig. 5B. The regressions on the data represented by the closed circles and by the open circles are shown as the solid and dashed lines, respectively. (B) Linear regressions on the low laser flash energy portion of the data shown in Fig. 5D. The symbols and flash energies are the same as in Fig. 5D and the regressions on the data represented by the closed circles, crosses, and open circles are shown as the solid, dashed, and dotted lines, respectively. (C) Calculated relationship between the apparent relative absorption cross-section measured at low laser flash energies and γ . The curves were calculated using $T = 4$, $\sigma = 1.0$ and $B = 0$. The values for A and γ are shown in the figure. Relative cross-sections (± 1 S.D.) obtained from the regressions presented in (A) and (B) are shown by the solid circles and crosses, respectively. The data have been normalized so that at $\gamma = 1.0$ the relative cross-sections are unity.

Effects of long-lived quenchers

In our calculations we assume that all the excited states created in a Unit during a flash decay independently. If photons absorbed in a Unit during the flash interact in annihilation events before encountering RCII, or form long-lived quenchers [48–56], our calculations will overestimate flash yields. However, bi-excitonic interactions cannot explain the flash saturation behavior observed in Fig. 5 because the power densities of our flashes are too low. For example, assume that a Unit consisting of four RCII and their antennae is illuminated with a 500 ns flash of energy equivalent to three photons absorbed per RCII. This flash energy (which would produce about 95% of the maximum flash yield) would, on the average, excite the Unit once every 40 ns. This excitation frequency exceeds the maximum *in vivo* fluorescence lifetime (about 2 ns [33–35]) by a factor of 20. Thus, even for flash energies near saturation, there is no more than one photon at any time in such a Unit.

An alternative possibility is that a single excitation arriving at a closed RCII can, with some probability, form a long-lived quencher (e.g., a carotenoid triplet [52–56]). We note that, if the probability of quencher formation is high, this process is equivalent to the case where A is small: an excitation arriving at a closed RCII does not escape, it either forms a quencher or is quenched. If a quencher is formed with low probability and if many RCII form a Unit, we might expect a decrease in flash yield (relative to the case of no quenching) to result at flash energies near satura-

tion when many excitations are present in Units in which most of the RCII are closed. We have tested for the possibility that our data have been influenced by the presence of long-lived quencher formation in two ways.

A low flash energies, where the population of quenchers should be negligible, flash yields are linearly proportional to flash energies [10]. Figs. 6A and 6B show the data from Fig. 5 (panels B and D, respectively) with laser flash energies replotted on a linear scale. Linear regressions on the data are shown by the lines. The slopes obtained from the regressions yield values for σ_{O_2} . In panel A, the solid line is the regression on the data shown by the closed circles ($\gamma = 1.0$) and the dashed line is the regression on the data shown by the open circles ($\gamma = 0.25$). Values for σ_{O_2} obtained from the regressions are $73 \pm 3 \text{ \AA}^2$ and $77 \pm 6 \text{ \AA}^2$, respectively.

Similarly, in panel B, the solid, dashed and dotted lines are the regressions on the data shown by the closed circles ($\gamma = 1.0$), the crosses ($\gamma = 0.30$), and the open circles ($\gamma = 0.07$). Values for σ_{O_2} obtained from these regressions are 75 ± 4 , 84 ± 10 and $84 \pm 4 \text{ \AA}^2$, respectively.

The solid curves in Fig. 6C show the expected relative change in σ plotted as a function of γ for the different values of A indicated. For these calculations, $T = 4$ and $B = 0$. The normalized results of the regressions plotted in Fig. 6A, B are also shown in Fig. 6C. Similar to the results presented in Fig. 5, the data do not support values for A greater than about 0.25. This result argues against quenching of excitations by long-lived quenchers formed at laser flash energies below saturation.

In a second set of experiments to test for long-lived quencher formation, we measured the change in the fluorescence yield of a dim, blue test flash given $30 \mu\text{s}$ following the actinic laser flash ($\Delta\phi(F30)$). $30 \mu\text{s}$ after a short flash all long-lived quenchers have decayed and RCII still remain in their closed state [48–50]. At this time the relative fluorescence yield is at its maximum [11,48–50].

Fig. 7 shows data from an experiment in which we simultaneously determined Y_{O_2} and $\Delta\phi(F30)$ as functions of the intensity of the actinic laser flash as described in Materials and Methods. the flash saturation behavior of Y_{O_2} is shown by the

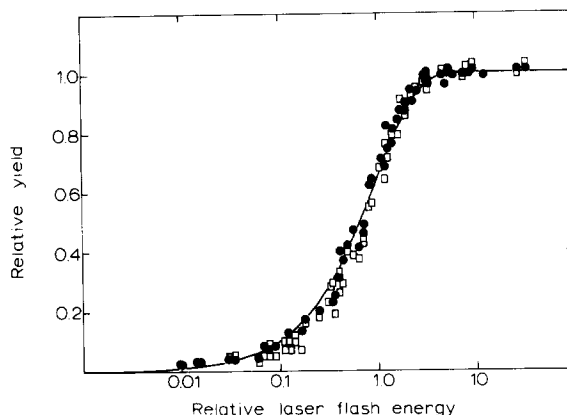


Fig. 7. Laser flash energy dependence of Y_{O_2} (closed circles) and $\Delta\phi(F30)$ simultaneously measured from *Chlorella* cells in the absence of background illumination. The laser flash frequency was 0.5 Hz. A relative laser flash energy of 1.0 corresponds to $0.79 \cdot 10^{14}$ quanta/cm². Cells (Chl/cell = 0.70 fmol, Chl b /Chl $b = 0.37$) were suspended in growth medium at a Chl concentration of $97 \mu\text{M}$. The curve drawn through the data was calculated using eqn. 3 with $\sigma_{O_2} = 110 \text{ \AA}^2$.

closed circles in Fig. 7. The open circles represent data for $\Delta\phi(F30)$. The solid curve shows a fit of Eqn. 3 to the Y_{O_2} data ($\sigma_{O_2} = 110 \text{ \AA}^2$). We note that the saturation curves described by Y_{O_2} and $\Delta\phi(F30)$ are similar, but not quite identical at low flash energies.

Y_{O_2} directly measures the fraction of RCII which has been closed by the actinic flash. $\Delta\phi(F30)$ allows us to probe the uninhibited system under conditions where γ is known and quenchers other than RCII are absent. Fig. 8 shows the data from Fig. 7 with $\Delta\phi(F30)$ plotted as a function of Y_{O_2} . $\Delta\phi(F30)$ is not a strictly linear function of Y_{O_2} . A fit of Eqn. 1 to these data yields $p = 0.18 \pm 0.02$. This fit is shown by the solid line and the 95% confidence limits are indicated by the dotted lines. The broken line corresponds to $p = 0.55$, the value obtained from the fit to the fluorescence induction data shown in Fig. 1.

The low values for p we obtain from the data shown in Figs. 7 and 8 support our preceding conclusion that A is small and argue against any significant effect on our results due to long-lived quenchers. The sharp contrast between the data shown in Figs. 1C and 8 provides an indication of how the simplifying assumptions used in the fluorescence induction analysis can lead to serious (300%!) error.

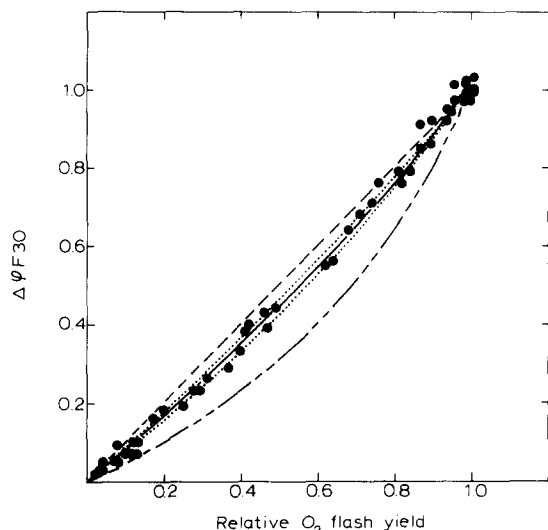


Fig. 8. $\Delta\phi(F30)$ plotted as a function of Y_{O_2} . The data are from Fig. 7. The curves were obtained using Eqn. 1 and correspond to $p = 0$ (dashed), $p = 0.18$ (solid), and $p = 0.55$ (broken). The two dotted curves show the 95% confidence limits on the fit to the data shown by the solid curve.

Effects of escape from open RCII

So far we have based our calculations and conclusions on the assumption that excitations do not escape from open traps ($B = 0$). Fig. 9 summarizes the effect that escape from open traps would have on our conclusions. For all the curves shown in Fig. 9, $T = 4$ and the solid and dashed curves correspond to $\gamma = 1.0$ and $\gamma = 0.05$, respectively. The three pairs of curves shown in panel A were obtained using different values for A and B . The curves have been displaced from one another along the flash energy (by varying σ) axis for clarity of presentation. In panel A, curves '1' were calculated using $B = 0$ and $A = 0.25$, curves '2' using $B = 0.25$ and $A = 0.50$, and curves '3' using $B = 0.60$ and $A = 0.75$.

All three of these curves provide fits comparable to those shown in Fig. 5 for $A = 0.25$ (which appears to be the upper limit for A and $B = 0$). However, as B becomes larger, the difference between A and B needed for a comparable fit becomes smaller. This is most clearly demonstrated by the curves shown in Fig. 9B. The curves labeled '1' were calculated using $B = 0.93$ and $A = 0.95$ and curves '2' using $B = 0.93$ and $A = 0.99$. Even though the difference in A is less than 5%, curves '1' could provide a reasonable fit to the

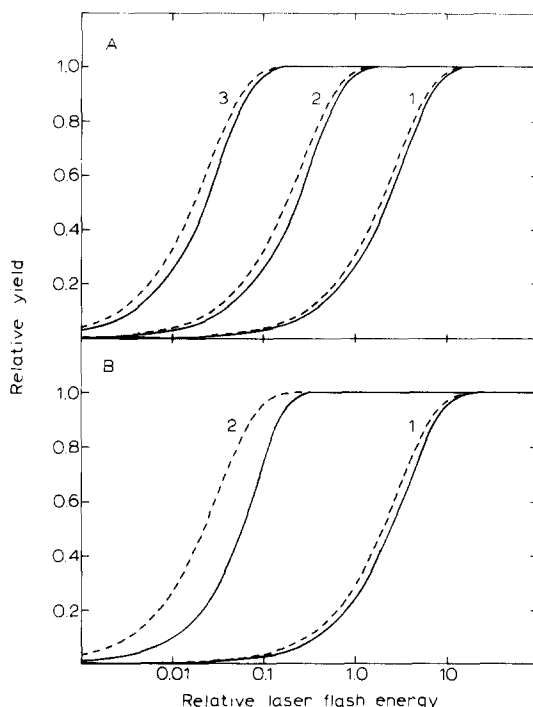


Fig. 9. Calculation of the effects of energy transfer from open RCII on the shape of the laser flash energy saturation curves. $\gamma = 1.0$ for solid curves and $\gamma = 0.95$ for dashed curves. Curves: (A) '1': $T = 4, \sigma = 0.30, A = 0.25, B = 0$. '2': $T = 4, \sigma = 3.0, A = 0.50, B = 0.25$. '3': $T = 4, \sigma = 30, A = 0.75, B = 0.60$. (B) '1': $T = 4, \sigma = 0.30, A = 0.95, B = 0.93$. '2': $T = 4, \sigma = 30, A = 0.99, B = 0.93$.

data shown in Fig. 5; curves '2' could not. In general, we can only obtain fits to our data when $(1 - B)/(1 - A) < 1.5$.

In light of the behavior of the curves shown in Fig. 9, we can conclude from our measurements that the difference, $A - B$, is small. The exact magnitude of this difference depends on the value of B . If B is small, our data permit us to conclude that $A < 0.25$. If B is significantly larger than 0, $A - B$ may be considerably smaller than 0.25. Finally, it is clear that, even if many RCII share antenna and even if A is large, when $B = A$ the effective antenna size available to open RCII will not change on closing RCII.

Discussion

Comparison of results obtained with continuous and flash illuminations

Measurements using continuous or pulsed il-

lumination techniques to determine the presence and extent of energy transfer among RCII give very different results. In this report we have used the same assay (fluorescence) and organism (*Chlorella*) and have measured the 'connection parameter', p [13,18,25], using both continuous illumination and short laser flashes. With continuous illumination we obtain a value for p (Fig. 1C, $p = 0.55$) that is 3-times greater than the value we obtain from the flash experiments (Fig. 8, $p = 0.18$). A small value for p is implied in all the results we have obtained with single-turnover flashes of light.

The interpretation of fluorescence induction kinetics is neither simple nor straightforward. The quantum yield of fluorescence is only indirectly related to RCII photochemistry and is known to be influenced by many factors other than the redox state of the reaction centers. A partial list of these includes: the physiological state of the organism [43,57], ion concentrations and fluxes [58–60], membrane potentials [60–63], and charge storage by the O_2 -evolving system [64,65]. The use of herbicides to prevent multiple turnovers by RCII introduces additional complications. There are reports that even high concentrations of DCMU do not completely stop electron transfer between RCII and the plastoquinone pool [28,29]. Furthermore, the presence of multiple acceptors in RCII may allow multiple turnovers in the presence of inhibitors [66–68]. Diner and Delosme [69] have recently found that the low potential fluorescence quencher (Q_L) is not associated with the transmembrane charge separation reaction in PSII, and is the result of a different photoreductive process in RCII. Finally, changes in the fluorescence yield occur on relatively long time-scales when RCII remain closed in the presence of inhibitors. Joliot and Joliot [70] have shown that, in the presence of DCMU, the fluorescence yield measured 3 ms after a saturating flash is 30–50% greater than the yield measured 20 μ s after the flash. Our own observations comparing F_m/F_0 measured with continuous light with that measured 30 μ s after a saturating single-turnover flash suggest similar changes in yield. An equivalent effect is evident in the data of Deprez et al. [56].

All of the points listed above directly relate to the assumptions used in the analysis of fluores-

cence induction as shown in Fig. 1. Qualitatively, it is clear that, under normal conditions, the fluorescence yield rises when RCII are closed. However, the exact quantitative relationships between the redox state of RCII and the yield of fluorescence, which are required for the analysis, remain to be resolved. In general, saturation behavior with continuous light depends on turnover times which may themselves be functions of illumination in photosynthetic systems.

Joliot et al. [14] measured rates of O_2 production by *Chlorella* cells partially inhibited with low concentrations of DCMU and illuminated with dim light. Rates of O_2 evolution were greater than expected from the fraction of open RCII (as assayed by a superimposed saturating flash). Joliot et al. interpreted this result as due to a nearly 3-fold increase in the antenna size for the open RCII when most of the RCII have been closed. In contrast, our direct measurements of σ_{O_2} (Figs. 5, 6) in *Chlorella* show no large changes, even when more than 90% of the RCII have been closed. The direct comparison of rates determined in continuous (or modulated) light and yields of single-turnover flashes can be troublesome. While flash yields measure instantaneous concentrations of donor and acceptor species, steady-state rates (continuous or modulated) measure throughput: a convolution of irradiance, absorption cross-sections, quantum yields and turnover times of multiple components with some in pools. As such, a larger number of factors can adversely influence the steady-state rates as compared to flash yields. It is interesting to note that when RCII are inhibited noncompetitively (with ultraviolet irradiation), a linear relationship between the rate of O_2 evolution and the fraction of open RCII is obtained [14].

We believe that the differences between the conclusions derived from experiments using pulsed and continuous illumination result from the fundamental differences between the two techniques. Rates observed using continuous illumination are necessarily complex convolutions of light absorption and reaction rates, turnover times, and often, the kinetics of unrelated processes. These complications can be eliminated or at least greatly reduced by the careful use of pulsed illumination conditions.

Energy transfer among RCII

Our major conclusion from the experiments described in this report is that, regardless of the number of RCII in a Unit, the quantity $A - B$ is small (less than 0.25 for $T > 2$). Thus there is no large change in quenching by RCII on conversion from the open to the closed state. Depending on the value of B , two extremes are obtained.

If $B = 0$, closed RCII can quench excitations with high yield (in the sense that the excited states are not available to other RCII). Thus, although many RCII may share a large antenna, there is little energy exchange among the RCII. We re-emphasize here that the conclusion that A is small does not necessarily imply either that the site of quenching is RCII or that there is no change in fluorescence lifetime when RCII are closed.

If $B > 0$, there is energy migration among RCII in the Unit, even when all RCII are open. However, if $A \approx B$, open and closed RCII are almost equally effective quenchers, there is little change in antenna size available to open RCII when any RCII in the Unit are closed.

Recently, Haehnel et al. [33,34] have described time-resolved measurements of fluorescence lifetimes and amplitudes from algae and isolated chloroplasts. These measurements have shown that the major part of the increase in fluorescence yield observed when RCII are closed in the presence of DCMU is due to the increase in amplitude of long-lived component of fluorescence emission. They have interpreted their results as indicating that the extent of energy transfer among RCII is small [34]. We have found similar results in time-resolved, double-flash experiments in which RCII are closed by light in the absence of inhibitors [35].

The common expectation based on the matrix model for photosynthesis is that when a substantial portion of the RCII in a Unit are closed, the remaining open RCII will perceive an increased antenna. We emphasize that this result will occur only if there is a large difference between escape of excitations from open and closed RCII. Our result that $A - B$ is small means that, no matter how many RCII share an antenna and no matter how great the degree of energy transfer among RCII may be, closing RCII does not greatly increase the cross-section of the remaining open RCII.

Paillotin et al. [32] have recently published a master equation theory to describe properties of photosynthetic domains. An important parameter in their model is the quantity R . They defined R as the ratio K_o/K_m , where K_o is the total rate of deactivation of singlet excitons in a domain with all RCII open and K_m is the rate all RCII are closed. Our result that $A - B$ is small is equivalent to the observation that R is small. The statement by Paillotin et al. that $R = F_m/F_0$ [32] rests on the assumptions that F_v and F_0 arise from the same process in PSII and that the only rate constant to change when RCII are closed is the decay constant for quenching. The recent picosecond fluorescence measurements [33–35] lend support to an alternative explanation, first proposed by Klimov et al. [72], that F_v represents a recombination luminescence from closed RCII. In light of this possibility and the discussion in the preceding section, we note that a large value for F_m/F_0 does not necessarily imply a large value for R , and equating the two parameters is probably unjustified.

Appendix

Calculation of flash energy saturation curves

We define a Unit to contain T RCII. C is the number of the RCII in a Unit which are closed. A and B are the probabilities of escape from closed and open traps as described in the text. We can calculate, by summing a series (as did Joliot and Joliot [13], a probability that an excitation is not trapped in a Unit having C closed traps:

$$P = \frac{(1-A)C/T}{1-B+(B-A)C/T} \quad (A1)$$

If $B = 0$

$$P_A = \frac{(1-A)C/T}{1-AC/T} \quad (A2)$$

and we recover the Joliot's equation. (Eqn. 1 in the text). If $A = 0$

$$P_B = \frac{C/T}{1-B(1-C/T)} \quad (A3)$$

and if $A = B$

$$P = C/T \quad (\text{A4})$$

there is no observable effect of the "escapes"!

Unfortunately, Eqns. A1–A4 do not take into account the consecutive nature of trapping and escape. If we define the probability of escape with adequate care (see text), the fraction of RCII closed (C/T) is not constant during the measurement. It changes as each trial is attempted. Thus the above equations, although widely used, are inadequate.

For these reasons we calculated flash energy saturation curves using a modified version of the iterative semiannihilation algorithm described by Mauzerall [23]. This calculation treats the properties of a large ensemble of Units and calculates the cumulative effects of successive photons absorbed by a Unit. Using the parameters A, B, C, T and γ as described previously, the iterative portion of the calculation is:

- (1) $H = E(1 - B)(T - C)/T$
- (2) $E = EAC/T + EB(T - C)/T$
- (3) $C = H + C$

The first line calculates the newly closed RCII, H , as the product of the excitation E , the probability of closing an open RCII ($1 - B$), and the fraction of open RCII $(T - C)/T$. Line (2) calculates the residual excitation as the sum of escape from closed (EAC/T) and from open ($EB(T - C)/T$) RCII. Line (3) updates the number of closed traps. At the start of the calculation, $E = 1$ (the first excitation absorbed by a Unit) and $C = (1 - \gamma)T$ (the number of RCII already closed at the time of the flash). The calculation cycles until E is small (less than 0.005). The yield of the first photon absorbed by the unit, Y_1 , (in terms of newly closed RCII: $C - ((1 - \gamma)T)$) is stored and the cycle is repeated using E reset to unity and the new value for C . Saturation curves are calculated as the products $Y_n P_n$. P_n , the probability that a Unit has absorbed exactly n photons during a flash, is calculated from the laser flash energy, the Unit absorption cross section, and the Poisson distribution [23,50]. All calculated curves are normalized to maximum flash yields of unity.

Acknowledgements

This work was supported by the U.S. Department of Agriculture contract number 5901941 9-03289 and by the National Science Foundation grant number PCM 83-16373.

References

- 1 Myers, J. and Graham, J.-R. (1971) *Plant Physiol.* 48, 282–236
- 2 Prezelin, B.A. and Alberte, R.S. (1978) *Proc. Natl. Acad. Sci. USA* 75, 1801–1804
- 3 Kawamura, M., Mimuro, M. and Fujita, Y. (1979) *Plant Cell Physiol* 20, 697–705
- 4 Melis, A. and Brown, J.S. (1980) *Proc. Natl. Acad. Sci. USA* 77, 4712–4716
- 5 Thielen, A.P.G.M. and Van Gorkom, H.J. (1981) *Biochim. Biophys. Acta* 635, 111–120
- 6 Myers, J., Graham, J.-R. and Wang, R.T. (1980) *Plant Physiol.* 66, 1144–1149
- 7 Falkowski, P.G., Owens, T.G., Ley, A.C. and Mauzerall, D.C. (1981) *Plant Physiol.* 68, 969–973
- 8 Melis, A. and Thielen, A.P.G.M. (1980) *Biochem. Biophys. Acta* 589, 275–286
- 9 Melis, A. and Anderson, J.M. (1983) *Biochem. Biophys. Acta* 724, 473–484
- 10 Ley, A.C. and Mauzerall, D.C. (1982) *Biochim. Biophys. Acta* 680, 95–106
- 11 Ley, A.C. and Mauzerall, D.C. (1982) *Biochim. Biophys. Acta* 680, 174–180
- 12 Ley, A.C. (1984) *Plant Physiol.* 74, 451–454
- 13 Joliot, A. and Joliot, P. (1964) *C.R. Acad. Sci. Paris* 258, 4622–4625
- 14 Joliot, P., Bennoun, P. and Joliot, A. (1973) *Biochim. Biophys. Acta* 305, 317–328
- 15 Melis, A. and Homann, P.H. (1976) *Photochem. Photobiol.* 23, 343–350
- 16 Melis, A. and Homann, P.H. (1978) *Arch. Biochem. Biophys.* 190, 523–530
- 17 Melis, A. and Duysens, L.N.M. (1979) *Photochem. Photobiol.* 29, 373–382
- 18 Bowes, J.M. and Horton, P. (1982) *Biochim. Biophys. Acta* 680, 127–133
- 19 Sonneveld, A., Rademaker, H. and Duysens, L.N.M. (1980) *Biochim. Biophys. Acta* 593, 272–289
- 20 Duysens, L.N.M. (1983) in *The Oxygen Evolving System of Photosynthesis* (Inoue, Y., Crofts, A.R., Govinjee, Murata, N., Renger, G. and Satoh, K., eds.), pp. 3–13, Academic Press, New York
- 21 Mauzerall, D. (1976) *Biophys. J.* 16, 87–91
- 22 Geacintov, N.E., Breton, J., Swenberg, C.E. and Paillotin, G. (1977) *Photochem. Photobiol.* 26, 629–638
- 23 Mauzerall, D. (1982) in *Biological Events Probed by Ultrafast Laser Spectroscopy* (Alfano, R., ed.), pp. 215–235, Academic Press, New York
- 24 Diner, B.A. and Wollman, F.-A. (1979) *Plant Physiol.* 63, 20–25

- 25 Mathis, P. and Paillotin, G. (1981) in *The Biochemistry of Plants*, Vol. 8, Photosynthesis (Hatch, M.D. and Boardman, N.K., eds.), pp. 97–161, Academic Press, New York
- 26 Wintermans, J.F.G.M. and DeMots, A. (1965) *Biochim. Biophys. Acta* 109, 448–453
- 27 Hodges, M. and Barber, J. (1983) *Plant Physiol.* 72, 1119–1122
- 28 Hodges, M. and Barber, J. (1983) *FEBS Lett.* 160, 177–181
- 29 Schreiber, U. and Pfister, K. (1982) *Biochim. Biophys. Acta* 680, 60–68
- 30 Joliot, P. and Joliot, A. (1979) *Biochim. Biophys. Acta* 546, 93–105
- 31 Paillotin, G. (1976) *J. Theor. Biol.* 58, 219–235, 237–252
- 32 Paillotin, G., Geacintov, N.E. and Breton, J. (1983) *Biophys. J.* 44, 65–77
- 33 Haehnel, W., Nairn, J.A., Reisberg, P. and Sauer, K. (1982) *Biochim. Biophys. Acta* 680, 161–173
- 34 Haehnel, W., Holzworth, A.R. and Wendler, J. (1973) *Photochem. Photobiol.* 37, 435–443
- 35 Mauzerall, D.C. (1985) *Biochim. Biophys. Acta* 809, 11–16
- 36 Collins, F.C. and Kimball, G.E. (1949) *J. Colloid Sci.* 4, 425–437
- 37 Avron, M. and Ben-Hayyim, B. (1969) in *Progress in Photosynthesis Research*, Vol. 3 (Metzner, H., ed.), pp. 1185–1196, University of Tübingen Press, Tübingen
- 38 Sun, A.S.K. and Sauer, K. (1971) *Biochim. Biophys. Acta* 234, 399–414
- 39 Cho, H.M., Manicino, C.J. and Blankenship, R.E. (1984) *Biophys. J.* 45, 455–462
- 40 Forbush, B., Kok, B. and McGloir, M.P. (1973) *Photochem. Photobiol.* 14, 307–321
- 41 Bennett, J. (1983) *Phil. Trans. R. Soc. Lond. B* 302, 113–125
- 42 Horton, P. (1983) *FEBS Lett.* 152, 47–52
- 43 Bonaventura, C. and Myers, J. (1969) *Biochim. Biophys. Acta* 189, 366
- 44 Horton, P. and M.T. Block (1981) *Biochim. Biophys. Acta* 635, 53–62
- 45 Steinbeck, K.E., Bose, S. and Kyle, D.J. (1982) *Arch. Biochem. Biophys.* 216, 356–351
- 46 Farchaus, J.W., Widger, D.R., Cramer, L.A. and Dilley, R.A. (1982) *Arch. Biochem. Biophys.* 217, 362–367
- 47 Bennett, J. (1980) *Eur. J. Biochem.* 104, 85–89
- 48 Mauzerall, D.C. (1972) *Proc. Natl. Acad. Sci. USA* 69, 1358–1362
- 49 Mauzerall, D.C. (1976) *J. Phys. Chem.* 80, 2306–2309
- 50 Mauzerall, D.C. (1981) *Proceedings of the 5th International Congresson Photosynthesis. I. Photophysical processes-Membrane Energization* (Akoyunoglou, G., ed.), pp. 47–58, Balaban International Sciences Services, Philadelphia
- 51 Geacintov, N.E., Breton, J., Swenberg, C.E. and Paillotin, G. (1977) *Photochem. Photobiol.* 26, 629–638
- 52 Mathis, P., Butler, W.L. and Satoh, K. (1979) *Photochem. Photobiol.* 30, 603–614
- 53 Maroti, P. and Laval, J. (1979) *Photobiol.* 30, 1147–1152
- 54 Kramer, H. and Mathis, P. (1980) *Biochim. Biophys. Acta* 593, 319–329
- 55 Breton, J., Geacintov, N.E. and Swenberg (1979) *Biochim. Biophys. Acta* 548, 616–635
- 56 Deprez, J., Dobek, A., Geacintov, N.E., Paillotin, G. and Breton, J. (1983) *Biochim. Biophys. Acta* 725, 444–454
- 57 Satoh, K. and Fork, D.C. (1983) *Photochem. Photobiol.* 37, 429–434
- 58 Hind, G. and McCarty, R.E. (1973) in *Photophysiology*, Vol. 8 (Giese, A.C., ed.), pp. 114–156, Academic Press, New York
- 59 Barber, J., Chow, J.S., Scoufflaire, C. and Lannoye, R. (1980) *Biochim. Biophys. Acta* 591, 92–103
- 60 Govindjee and Papageorgiou, G. (1971) in *Photophysiology*, Vol. 6 (Giese, A.C., ed.), pp. 1–46, Academic Press, New York
- 61 Jennings, R.C., Garlaschi, F.M. and Forti, G. (1976) *Biochim. Biophys. Acta* 423, 264–274
- 62 Chow, W.S., Telfer, A., Chapman, D.J. and Barber, J. (1981) *Biochim. Biophys. Acta* 638, 60–68
- 63 Satoh, K. and Fork, D.C. (1983) *Photosynthesis Res.* 4, 61–70
- 64 Joliot, P. and Joliot, A. (1971) in *Proceedings of the 2nd International Congress on Photosynthesis Research*, Stresa, Volume 1, pp. 26–38, Dr. W. Junk, the Hague
- 65 Delosme, R. (1971) in *Proceedings of the 2nd International Congress on Research*, Stresa, Volume 1, pp. 187–195, Dr. W. Junk, The Hague
- 66 Morin, P. (1964) *J. Chim. Biol.* 61, 624–680
- 67 Lavorel, J. (1972) *C.R. Acad. Sci. Paris Ser. D*, 274, 2902–2912
- 68 Doschek, W. and Kok, B. (1972) *Biophys. J.* 12, 832–838
- 69 Diner, B.A. and Delosme, R. (1983) *Biochim. Biophys. Acta* 722, 443–451
- 70 Joliot, P. and Joliot, A. (1977) *Biochim. Biophys. Acta* 462, 559–574
- 71 Vermaas, W.F.J., Dohnt, G. and Renger, G. (1984) *Biochim. Biophys. Acta* 765, 74–83
- 72 Klimov, V.V., Allskheverdiev, and Pashernko, V.Z. (1978) *Dokl. Akad. Nauk. USSR* 244, 1204–1207